Energy Transfer Mechanisms and Dopant-Dependent Luminescence Properties of Er-ZnO Nanoparticles

C.JAYACHANDRAIAH[a*], K. SIVA KUMAR[b], Sunilkumar.A[c]

[a]Undergraduate Programme, Indian Institute of Science Bangalore-560 012, India

[b]Department of Physics, School of Technology, The Apollo University, Chittoor, A.P, 517127 India.

[c]Department of physics, Ballari Institute of Technology and Management, Ballari -583104, India

ABSTRACT:

Pure and Er (1.30, 1.79, 2.83 and 3.53 at. %) doped ZnO nanoparticles have been synthesized by chemical co-precipitation method. The synthesized samples were characterized by powder X-ray diffraction (XRD), transmission electron microscopy (TEM), thermo gravimetric analysis (TGA) for thermal stability, Fourier transform infrared (FTIR) spectroscopy and photoluminescence (PL) studies. The XRD measurements confirmed the hexagonal wurtzite structure of ZnO for all samples. The crystallite size of the samples decreases with increase in concentration and are compatible with the results obtained from TEM analysis. TGA analysis of the samples reveals fine thermal stability with no significant weight loss. The shifting of ZnO stretching mode from the FTIR spectra confirm the substitution of Er in ZnO host. The PL emission spectra of pure and Er doped ZnO nanoparticles exhibit similar visible emission bands with excitation wavelength 340 nm and 367 nm. However, small near band edge (UV) emissions at 387 and 398 nm are observed with excitation wavelength 340 nm. The maximum broad band green emission is detected for 1.30 at. % of Er. The auxiliary green band (GB) emissions at 523 nm, 531nm and red band emission at 650 nm confirm the presence of Er in ZnO host.

Keywords: Erbium; Zinc Oxide nanoparticles; Photoluminescence; XRD; TGA

1. INTRODUCTION

Nanometre-scale materials and semiconductors in particular seem to be important and promising in the development of next-generation electronic and optoelectronic devices [1-3]. Among these ZnO receives much interest due to its wide direct band gap (3.4 eV) and huge excitation binding energy (60 meV) [4]. It is a multifunctional semiconductor as it can be utilized as photo catalytic, optoelectronic, piezoelectric, gas sensing and luminescence devices etc. [5-10].

The optical, electrical and magnetic properties of ZnO nanoparticles can be easily tuned by doping the transition elements [11, 12] and rare earth elements [13, 14].

Owing to unique optical properties rare-earth doped semiconducting materials [15, 16] have been of great scientific interest in photonic devices and flat-panel displays, which needs high-efficiency fluorescence materials to improve their qualities [17] due to their 4f electronic configuration. Particularly trivalent state erbium (Er^{3+}, $4f^{11}$) doped semiconductor nanostructures have been extensively studied due to optical intra-4f transitions at 1.54 μm ($^4I_{13/2} \rightarrow {}^4I_{15/2}$) for telecommunication [18]. It can also be used for up conversion luminescence and down conversion luminescence properties due to its favorable electronic energy levels [19].

In this research work we report, on the structural, thermal, and photoluminescence properties of Er-doped ZnO nanoparticles. Though rare earthed doped ZnO nanoparticles can be synthesized by many techniques such as forced hydrolysis, pulsed laser deposition, micro emulsion tem plating etc. [20-22], we adopted wet chemical co-precipitation method as it is easily reproducible and less expensive. By virtue of the optical spectra of Er^{3+} in the present study, we can explicitly prove the existence of multiple luminescence centers of Er^{+} in ZnO nanoparticles.

2. EXPERIMENTAL

Er doped ZnO nanoparticles were prepared by a facile co-precipitation method. A high purity (99.9 %) analytical reagent (AR) grade chemicals; Zinc acetate ($Zn(CH_3COO)_2 . 2H_2O$) and erbium chloride hexahydrate (Cl_3 Er $6H_2O$) were the starting materials obtained from Sigma-Aldrich Company. Here, the dopant, erbium concentration was varied at 1.30, 1.79, 2.83 and 3.53 at. % in the host matrix. Appropriate quantity of precursors was dissolved in Ethanol- deionized water (50-50 %) with polyvinylpyrrolidone (PVP) as a surfactant and stirred for 30 min until clear solution is formed. Then, the NaOH is added to have optimum nucleation at p^H-9. This solution was transformed to hot bath of temperature 90°C and stirred rigorously for 4 hours to get fine precipitation. As formed precipitation was washed 4 times with de-ionized water and centrifuged. The precipitation was collected and dried at 80°C for 4 hours.

The as-prepared samples were investigated systematically using the following analytical techniques. The composition of the prepared samples was analyzed through X-ray diffraction (XRD) measurements (D8 Advance, Bruker, Germany) for structure analysis. The morphology was inspected by transmission electron microscope (TEM) of JEM-100CX. The functional groups analysis was carried out by Bruker Alpha-T FT-IR Spectrometer. The thermal stability of the

samples was studied using TGA/DTA analysis (EXSTAR TG/DTA 630) in air atmosphere at a scan rate of 5ºC/min. Photoluminescence spectra were recorded in the wavelength range of 300-800 nm using FP-8500, JASCO Spetrofluorimeter with a Xe-arc lamp of power 60W.

3. RESULT AND DISCUSSION

3.1. Structural, morphological and compositional analysis

XRD patterns of undoped and Er doped ZnO nanoparticles are shown in **Fig. 1**. All the diffraction peaks could be well indexed to reflections from the (100), (002), (101), (102), (110), (103), and (112) planes of the hexagonal wurtzite structure of ZnO (JCPDS card no. 36-1451). No characteristic peaks of other impurities such as Zn $(OH)_2$ or Er_2O_3 are observed. The average crystallite size (D) of the nanoparticles is determined by applying the following Scherrer equation,

$$D = \frac{k\lambda}{\beta cos\theta} \quad (1)$$

where k is the shape factor (0.89), λ is the wavelength of Cu K_α radiation (1.542 Å), β is the full width at half maxima intensity (FWHM) of the (101) diffraction peak (radians), θ is the Bragg's angle (half of the peak position angle). The calculated average crystallites size of the pure and Er doped ZnO nanoparticles are tabulated in **Table. 1**. The broadening and decrease in the intensity of diffraction peaks with increasing the doping concentration strongly suggest the successfully substitution of Er^{3+} in the ZnO host. Furthermore, the positions of diffraction peaks of Er doped ZnO samples show a slight shift towards the lower angle side due to ionic radius mismatch between host and dopant [23]. The micro-strain (ε) of Er-doped ZnO particle was calculated using the following formula [24]

$$\text{Micro-strain} \quad (\varepsilon) = \frac{\beta cos\theta}{4} \quad (2)$$

The increase in micro-strain may be due to the presence of defects and vacancies in the Er–Zn–O lattice [25-27]. The substitution of Er^{3+} interstitial would affect the concentration of the interstitial (O_i), oxygen vacancies (V_O) and interstitial (Zn_i), vacancies (V_{Zn}) [28].

The morphology of undoped and 2.83 at. % of Er doped ZnO nanoparticles were characterized by TEM and shown in **Fig. 2(a) and 2(b).** From the figure, it can be seen that the pure and Er-doped ZnO nanoparticles are similar and having virtually spherical morphology with an average diameter of 20-30 nm. The observed values are close to that of those estimated by Sherrer's equation in the XRD. However, the presence of Er in ZnO, enhances the agglomeration of the nanoparticles compared to undoped ZnO.

3.2. Fourier transform infrared (FTIR) studies

The chemical bonding information of the prepared samples was obtained by the FTIR technique. The characteristic peaks exhibited by FTIR spectra of pure and Er doped ZnO nanoparticles were shown in **Fig. 3**. The broad absorption peak at around 3435-3445 cm^{-1} is attributed to the normal O–H stretching vibration of H_2O in Er–Zn–O lattice which may be due to moisture in the solution and the atmosphere. The pure ZnO nanoparticles exhibit minor characteristic peaks at about 2930-2916 cm^{-1} and it could be ascribed to the $–CH_2–$ stretching vibration that arises from the precursor solution of ethanol. Another sharp peak at ~1576-1558 cm^{-1} is attributed to H–O–H bending vibration and is accompanied by in-plane deformation vibrations at ~1626-1639 cm^{-1}, which is assigned to the presence of H_2O in the ZnO nanoparticles. The observed peak at 1017 cm^{-1} is due to the C–O–C bond. The predictable Zn–O bond was observed at 498 cm^{-1} for pure ZnO (x=0.00) and this band was shifted towards lower frequency region from 497 cm^{-1} to 485 cm^{-1} for Er (1.30, 1.79, 2.83 and 3.53 at. %) doped ZnO nanoparticles. This may be due to the presence of Er^{3+} ions in the ZnO host matrix. The existence of C=O, C–O, $–CH_2–$ and C–O–C groups are originated from Zinc acetate dihydrate (Zn $(CH_3CO_2)_2$ $2H_2O$), ethanol (C_2H_5OH) and water (H_2O).

3.3. TGA analysis

Fig. 4 shows the TGA curves of undoped and Er doped ZnO nanoparticles in the temperature range 30-800ºC. From the figure, it is noticed that the weight insignificant loss ranging 3-8% with increase in dopant concentration. Increase of Er content in ZnO enhances the presence of volatile functional groups (such as OH, C=O, etc. due to low temperature synthesis) which undergo weight loss with temperature. The weight loss occurred in two steps for all samples. The first weight loss between 30 and 210°C is attributed to the removal of physically adsorbed water and chemically bound groups on the surfaces of prepared samples. The other weight loss was observed between 210 and 450°C corresponding to the removal of organic compound and the decomposition of other residual ions as indicated by FTIR spectra. Therefore, it is evidenced from the TGA curves that the ZnO nanoparticles were crystallized without significant loss.

3.4. Photoluminescence studies

The optical properties of ZnO nanoparticles can be influenced by the incorporation Er ions. Hence, the photoluminescence behavior of pure and Er doped ZnO nanoparticles were studied.

Fig. 5(a) and 5**(b)** show room temperature PL emission spectra with excitation wavelength 340 nm and 367 nm. The emission spectra of Er (1.30, 1.79, 2.83 and 3.53 at. %) doped ZnO nanoparticles are similar to that of pure ZnO nanoparticles with slender shift in visible region defective emission centers at~ 411 nm, 436 nm, 468 nm and 557 nm. However, two minor peaks at 387nm and 398 nm in the ultra-violet (UV) region are observed in the emission spectra with excitation 340 nm as shown in the inset of **Fig. 5(a)**. The UV emissions at 387 nm and 398 nm is associated with the excitonic (electron-hole pair) recombination corresponding to the near band edge emission of ZnO nanoparticles. These excitons recombination occurs at below near band edge excitation wavelength 362 nm. The violet- blue emission centers around 411 nm is due to the electron transition from the zinc interstitial (Zn_i) level to the valence band (VB) and the blue emission at 436 nm attributes to Zn_i along with OH^-ions present at surface of nanoparticles which are consistent with FTIR results and the peak at 468 nm correspond to the transition of ionized oxygen vacancy (V_O) to VB [36]. Finally, the broad level green emission at around 557 nm in the range 480 nm - 580 nm attributed to the recombination of electrons trapped in the holes of deep level single ionized oxygen vacancies (V_O^+) [37]. Along with these emissions small additional peaks are identified on broad band green emission at ~516 nm, 539 nm and a red emission at ~650 nm with increasing Er content which originate from 4f transitions of Er dopant, which can be explained as fallow.

When some excited ZnO(s) are trapped by broad defect levels, a part of recombination energy is transferred to the Er^{3+} ions to promote the Er^{3+} ions from ground state ($^4I_{15/2}$) to excited states ($^4F_{7/2}$, $^2H_{11/2}$, $^4F_{9/2}$) which causes additional peaks in green emission center in Er doped ZnO nanoparticles [34, 35, 38,39]. The transition ($^4F_{7/2}$, $^2H_{11/2}$, $^4F_{9/2}$) $\rightarrow ^4I_{15/2}$ gives green emission centers at ~516 nm, 539 nm and 650 nm. The broad level green emission intensity is observed to be optimum for 1.30 at. % of Er dopant in our experimental conditions. Thereafter, as Er content is increased from 1.79 to 3.53 at. %, the defective emission intensity gradually decreases but the sharpness of additional Er emission peaks are enhanced up to 2.83 at.%. As the energy transfer rate increases with increasing Er content quenches the visible defective emission and enhance the sharpness of additional peaks. It is also observed that the direct excitation of Er ion is increased at higher excitation wavelengths and concentrations. The Er emission centers were almost dominated

over defect centers at 400 nm excitation at 2.83 at. % of Er shown in **Fig. 6**. These results confirm the incorporation of Er ion into the lattice of ZnO.

4. CONCLUSION

The pristine and Er doped ZnO nanoparticles have been successfully synthesized by chemical co-precipitation method. All samples were crystallized in the hexagonal wurtzite structure of ZnO without any impurity phases. The substitution of Er in the ZnO nanoparticles is confirmed by EDS and FTIR spectra. The enhanced green emission is observed for 1.5 at. % of Er doped ZnO nanoparticles while the emission intensity is decreased with increasing Er content. However, the additional peaks at 516 nm, 532 nm, and 650 nm were originated from excited states ($^4F_{7/2}$, $^2H_{11/2}$, $^4F_{9/2}$) to ground state ($^4I_{15/2}$) of Er ions and their sharpness was increased with increasing excitation wavelength and Er content as well.

REFERENCES

1. M. Nirmal and L. Brus, "Luminescence Photophysics in Semiconductor Nanocrystals," *Accounts of Chemical Research*, vol. 32, no. 5, pp. 407–414, Nov. 1998, doi: https://doi.org/10.1021/ar9700320.
2. A. P. Alivisatos, "Semiconductor Clusters, Nanocrystals, and Quantum Dots," *Science*, vol. 271, no. 5251, pp. 933–937, Feb. 1996, doi: https://doi.org/10.1126/science.271.5251.933.
3. S. Kumar and P.D. Sahare, "Nd-doped ZnO as a multifunctional nanomaterial," *Journal of Rare Earths*, vol. 30, no. 8, pp. 761–768, Aug. 2012, doi: https://doi.org/10.1016/s1002-0721(12)60126-4.
4. Y. S. Park, C. W. Litton, T. C. Collins, and D. C. Reynolds, "Exciton Spectrum of ZnO," *Physical Review*, vol. 143, no. 2, pp. 512–519, Mar. 1966, doi: https://doi.org/10.1103/physrev.143.512.
5. T.-H. Moon, M.-C. Jeong, W. Lee, and Jae-Min Myoung, "The fabrication and characterization of ZnO UV detector," *Applied Surface Science*, vol. 240, no. 1–4, pp. 280–285, Aug. 2004, doi: https://doi.org/10.1016/j.apsusc.2004.06.149.
6. R. Y. Hong *et al.*, "Synthesis, surface modification and photocatalytic property of ZnO nanoparticles," *Powder Technology*, vol. 189, no. 3, pp. 426–432, Feb. 2009, doi: https://doi.org/10.1016/j.powtec.2008.07.004.
7. Atsushi Tsukazaki *et al.*, "Repeated temperature modulation epitaxy for p-type doping and light-emitting diode based on ZnO," *Nature Materials*, vol. 4, no. 1, pp. 42–46, Dec. 2004, doi: https://doi.org/10.1038/nmat1284.
8. Ü. Özgür *et al.*, "A comprehensive review of ZnO materials and devices," *Journal of Applied Physics*, vol. 98, no. 4, p. 041301, Aug. 2005, doi: https://doi.org/10.1063/1.1992666.
9. B. N. Jin, Sang Cheol Bae, S. H. Lee, and S-A. Im, "Effects of native defects on optical and electrical properties of ZnO prepared by pulsed laser deposition," *Materials Science and Engineering B,* vol. 71, no. 1–3, pp. 301–305, Feb. 2000, doi: https://doi.org/10.1016/s0921-5107(99)00395-5.

10. L. Irimpan, V. P. N. Nampoori, P. Radhakrishnan, A. Deepthy, and B. Krishnan, "Size dependent fluorescence spectroscopy of nanocolloids of ZnO," *Journal of Applied Physics*, vol. 102, no. 6, Sep. 2007, doi: https://doi.org/10.1063/1.2778637.
11. S. Muthukumaran and R. Gopalakrishnan, "Structural, FTIR and photoluminescence studies of Cu doped ZnO nanopowders by co-precipitation method," *Optical Materials*, vol. 34, no. 11, pp. 1946–1953, Sep. 2012, doi: https://doi.org/10.1016/j.optmat.2012.06.004.
12. V. K. Sharma, M. Najim, A. K. Srivastava, and G. D. Varma, "Structural and magnetic studies on transition metal (Mn, Co) doped ZnO nanoparticles," *Journal of Magnetism and Magnetic Materials*, vol. 324, no. 5, pp. 683–689, Mar. 2012, doi: https://doi.org/10.1016/j.jmmm.2011.08.061.
13. R.S. Ajimsha, A. K. Das, B. N. Singh, P. Misra, and L. M. Kukreja, "Structural, electrical and optical properties of Dy doped ZnO thin films grown by buffer assisted pulsed laser deposition," *Physica E Low-dimensional Systems and Nanostructures*, vol. 42, no. 6, pp. 1838–1843, Feb. 2010, doi: https://doi.org/10.1016/j.physe.2010.02.005.
14. T. Ohtake, S. Hijii, N. Sonoyama, and T. Sakata, "Electrochemical luminescence of n-type ZnO semiconductor electrodes doped with rare earth metals under the anodic polarization," *Applied Surface Science*, vol. 253, no. 4, pp. 1753–1757, Dec. 2006, doi: https://doi.org/10.1016/j.apsusc.2006.03.008.
15. M. Subramanian *et al.*, "Investigations on the structural, optical and electronic properties of Nd doped ZnO thin films," *Journal of Physics D*, vol. 42, no. 10, pp. 105410–105410, Apr. 2009, doi: https://doi.org/10.1088/0022-3727/42/10/105410.
16. W. Chen and J. Zhang, "Using Nanoparticles to Enable Simultaneous Radiation and Photodynamic Therapies for Cancer Treatment," *Journal of Nanoscience and Nanotechnology*, vol. 6, no. 4, pp. 1159–1166, Apr. 2006, doi: https://doi.org/10.1166/jnn.2006.327.
17. V. Z. Mordkovich, H. Hayashi, Masamitsu Haemori, Tomoteru Fukumura, and M. Kawasaki, "Discovery and Optimization of New ZnO-Based Phosphors Using a Combinatorial Method," *Advanced Functional Materials*, vol. 13, no. 7, pp. 519–524, Jul. 2003, doi: https://doi.org/10.1002/adfm.200304335.
18. A. Polman, "Erbium as a probe of everything?," *Physica B: Condensed Matter*, vol. 300, no. 1–4, pp. 78–90, Jul. 2001, doi: https://doi.org/10.1016/s0921-4526(01)00573-7.
19. K. Zhong, J. Xu, J. Su, and Y. lin Chen, "Upconversion luminescence from Er-N codoped of ZnO nanowires prepared by ion implantation method," *Applied Surface Science*, vol. 257, no. 8, pp. 3495–3498, Feb. 2011, doi: https://doi.org/10.1016/j.apsusc.2010.11.055.
20. X. Wang, X. Kong, Y. Yu, Y. Sun, and H. Zhang, "Effect of Annealing on Upconversion Luminescence of ZnO:Er^{3+} Nanocrystals and High Thermal Sensitivity," *Journal of Physical Chemistry C*, vol. 111, no. 41, pp. 15119–15124, Sep. 2007, doi: https://doi.org/10.1021/jp0686689.
21. B. G. Mishra and G. R. Rao, "Promoting effect of CeO2 on cyclohexanol conversion over CeO2-ZnO mixed oxide materials prepared by amorphous citrate process," *Bulletin of Materials Science*, vol. 25, no. 2, pp. 155–162, Apr. 2002, doi: https://doi.org/10.1007/bf02706236.

22. A. Ishizumi and Y. Kanemitsu, "Structural and luminescence properties of Eu-doped ZnO nanorods fabricated by a microemulsion method," *Applied Physics Letters*, vol. 86, no. 25, Jun. 2005, doi: https://doi.org/10.1063/1.1952576.
23. Y. Chen, X. L. Xu, G. H. Zhang, H. Xue, and S. Y. Ma, "Blue shift of optical band gap in Er-doped ZnO thin films deposited by direct current reactive magnetron sputtering technique," *Physica E: Low-dimensional Systems and Nanostructures*, vol. 42, no. 5, pp. 1713–1716, Mar. 2010, doi: https://doi.org/10.1016/j.physe.2010.01.029.
24. P. P. Hankare, P. A. Chate, D. J. Sathe, P. A. Chavan, and V. M. Bhuse, "Effect of thermal annealing on properties of zinc selenide thin films deposited by chemical bath deposition," *Journal of Materials Science: Materials in Electronics*, vol. 20, no. 4, pp. 374–379, May 2008, doi: https://doi.org/10.1007/s10854-008-9736-8.
25. S. Kulal, S. Rau, and Bamane, "Synthesis of Cerium doped Zinc oxide nanoparticles by aqueous hydrothermal method and study of their properties," *Archives of Applied Science Research*, vol. 2, no. 6, pp. 205–210, 2010, Available: https://www.scholarsresearchlibrary.com/articles/synthesis-of-cerium-doped-zinc-oxide-nanoparticles-by-aqueous-hydrothermal-method-and-study-of-their-properties.pdf
26. K. Winer, "Chemical-equilibrium description of the gap-state distribution ina-Si:H," *Physical Review Letters*, vol. 63, no. 14, pp. 1487–1490, Oct. 1989, doi: https://doi.org/10.1103/physrevlett.63.1487.
27. H. Schmalzried, "F. A. Kröger: *The Chemistry of Imperfect Crystals*, North-Holland Publishing Company-Amsterdam 1964. 1039 Seiten. Preis: hfl. 110,-.," *Berichte der Bunsengesellschaft für physikalische Chemie*, vol. 68, no. 6, pp. 608–608, Aug. 1964, doi: https://doi.org/10.1002/bbpc.19640680615.
28. X. Peng, J. Xu, H. Zang, B. Wang, and Z. Wang, "Structural and PL properties of Cu-doped ZnO films," *Journal of Luminescence*, vol. 128, no. 3, pp. 297–300, Mar. 2008, doi: https://doi.org/10.1016/j.jlumin.2007.07.016.
29. N. Goswami and Dhirendra Kumar Sharma, "Structural and optical properties of unannealed and annealed ZnO nanoparticles prepared by a chemical precipitation technique," *Physica E: Low-dimensional Systems and Nanostructures*, vol. 42, no. 5, pp. 1675–1682, Mar. 2010, doi: https://doi.org/10.1016/j.physe.2010.01.023.
30. R. Y. Hong *et al.*, "Synthesis, surface modification and photocatalytic property of ZnO nanoparticles," *Powder Technology*, vol. 189, no. 3, pp. 426–432, Feb. 2009, doi: https://doi.org/10.1016/j.powtec.2008.07.004.
31. R. Saleh, S. P. Prakoso, and A. Fishli, "The influence of Fe doping on the structural, magnetic and optical properties of nanocrystalline ZnO particles," *Journal of Magnetism and Magnetic Materials*, vol. 324, no. 5, pp. 665–670, Mar. 2012, doi: https://doi.org/10.1016/j.jmmm.2011.07.059.
32. S. Muthu Kumaran and R. Gopalakrishnan, "Structural, optical and photoluminescence properties of Zn1−xCexO (x = 0, 0.05 and 0.1) nanoparticles by sol–gel method annealed under Ar atmosphere," *Journal of Sol-Gel Science and Technology*, vol. 62, no. 2, pp. 193–200, Feb. 2012, doi: https://doi.org/10.1007/s10971-012-2708-8.

33. Jörg. J. Schneider *et al.*, "Synthesis, Characterization, Defect Chemistry, and FET Properties of Microwave-Derived Nanoscaled Zinc Oxide," *Chemistry of Materials*, vol. 22, no. 7, pp. 2203–2212, Mar. 2010, doi: https://doi.org/10.1021/cm902300q.
34. S. Ji, L. Yin, G. Liu, L. Zhang, and C. Ye, "Synthesis of Rare Earth Ions-Doped ZnO Nanostructures with Efficient Host−Guest Energy Transfer," *The Journal of Physical Chemistry C*, vol. 113, no. 37, pp. 16439–16444, Aug. 2009, doi: https://doi.org/10.1021/jp906501n.
35. Y. Chen, X. L. Xu, G. H. Zhang, H. Xue, and S. Y. Ma, "Blue shift of optical band gap in Er-doped ZnO thin films deposited by direct current reactive magnetron sputtering technique," *Physica E: Low-dimensional Systems and Nanostructures*, vol. 42, no. 5, pp. 1713–1716, Mar. 2010, doi: https://doi.org/10.1016/j.physe.2010.01.029.
36. B. Jin and D. Wang, "Strong violet emission from zinc oxide dumbbell-like microrods and nanowires," *Journal of Luminescence*, vol. 132, no. 8, pp. 1879–1884, Aug. 2012, doi: https://doi.org/10.1016/j.jlumin.2012.03.026.
37. Seung Yong Bae, Chan Woong Na, Ja Hee Kang, and J. Park, "Comparative Structure and Optical Properties of Ga-, In-, and Sn-Doped ZnO Nanowires Synthesized via Thermal Evaporation," *The Journal of Physical Chemistry B*, vol. 109, no. 7, pp. 2526–2531, Jan. 2005, doi: https://doi.org/10.1021/jp0458708.
38. Y.-P. Du, Y.-W. Zhang, L.-D. Sun, and C.-H. Yan, "Efficient Energy Transfer in Monodisperse Eu-Doped ZnO Nanocrystals Synthesized from Metal Acetylacetonates in High-Boiling Solvents," *The Journal of Physical Chemistry C*, vol. 112, no. 32, pp. 12234–12241, Jul. 2008, doi: https://doi.org/10.1021/jp802958x.
39. Z. Pan *et al.*, "Er-doped ZnO films grown by pulsed e-beam deposition," *Journal of Physics: Condensed Matter*, vol. 19, no. 26, p. 266216, Jun. 2007, doi: https://doi.org/10.1088/0953-8984/19/26/266216

Tables with captions:

Sample ZnO:Er	Diffraction angle(2θ)	FWHM (β)	Particle size (D) nm	Micro-strain (ε) (10^{-3})	Relative peak intensity(%)
0 at. %	36.300	0.3378	24.47	1.4006	100
1.30 at. %	36.298	0.3890	21.56	1.6129	68
1.79 at. %	36.297	0.4033	20.49	1.6722	59
2.83 at. %	36.296	0.4568	18.10	1.8940	56
3.53 at. %	36.295	0.4854	17.03	2.0126	50

Table 1. Diffraction angle, average particles size, micro strain of pure and Er doped ZnO nanoparticles.

Assignments of ZnO:Er	Wave number (cm^{-1})					Reference no.
	0 at. %	1.32 at. %	1.79 at. %	2.82 at. %	3.52 at. %	
O–H stretching	3429	3431	3435	3442	3445	[28,31]
$–CH_2–$ stretching	2930	2921	2916	----	2916	[29]
H–O–H bending vibration	1626	1632	1637	1639	1639	[33]
H–O–H bending vibration	1576	1568	1561	1560	1558	[28]
Symmetric stretching C=O mode	1405	1410	1412	1412	1412	[31]
C–O–C bond	1017	1017	1017	1017	1017	[32]
Zn–O bond	498	497	492	491	485	[31,33]

Table 2. Functional group analysis of pure and Er doped ZnO nanoparticles from FTIR spectra.

Figures with captions

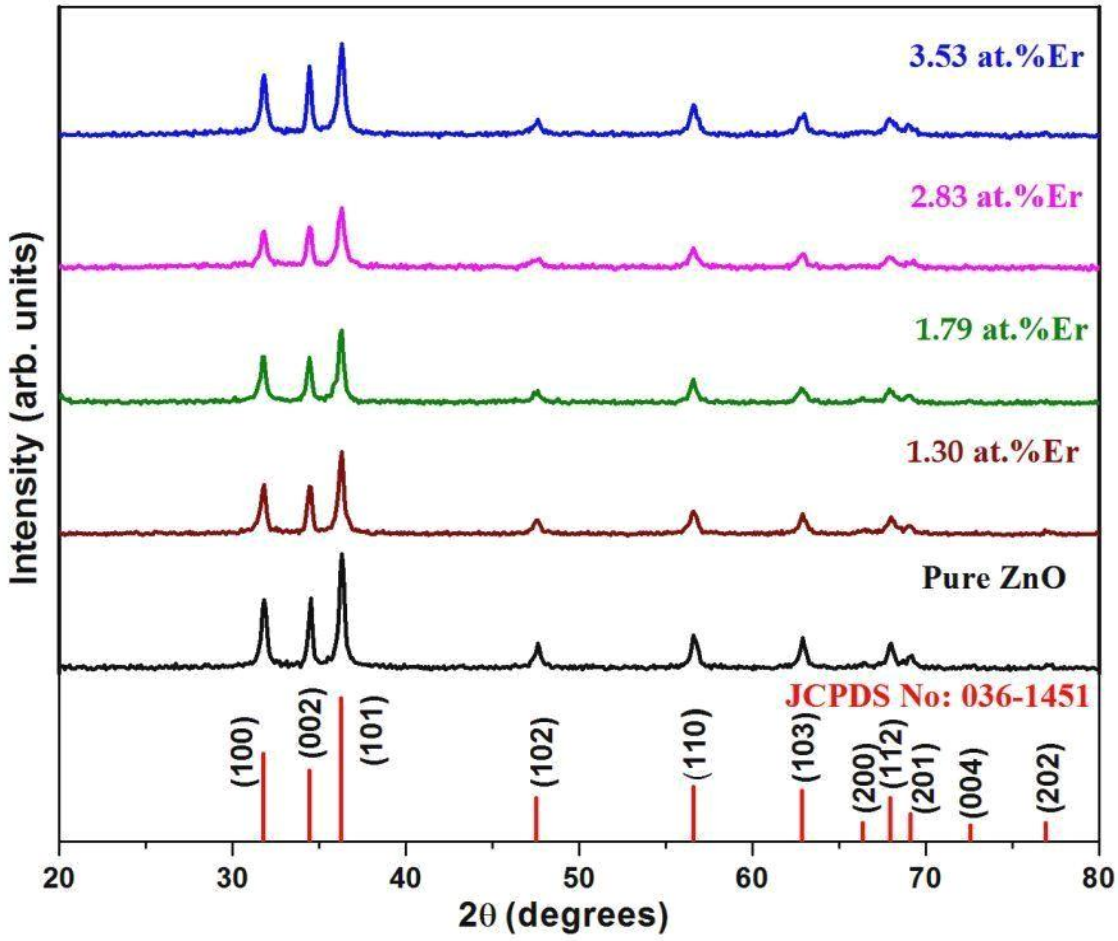

Fig. 1. XRD patterns of undoped and Er doped ZnO nanoparticles

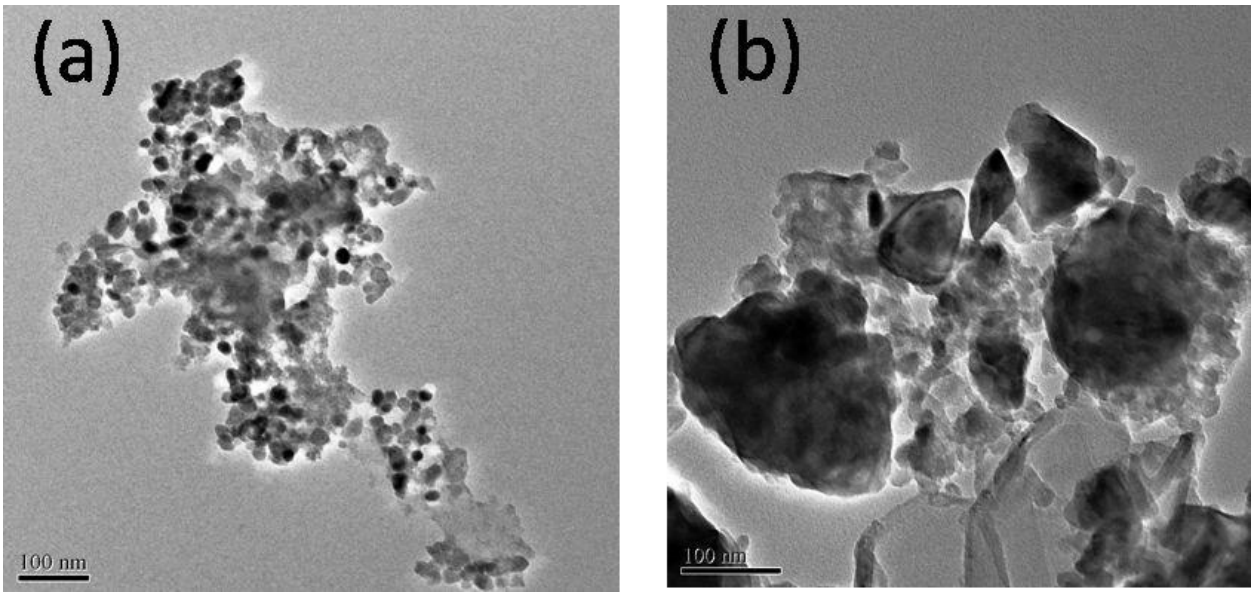

Fig. 2. Typical TEM images of (a) pure ZnO and (b) 3 at. % Er doped ZnO nanoparticles.

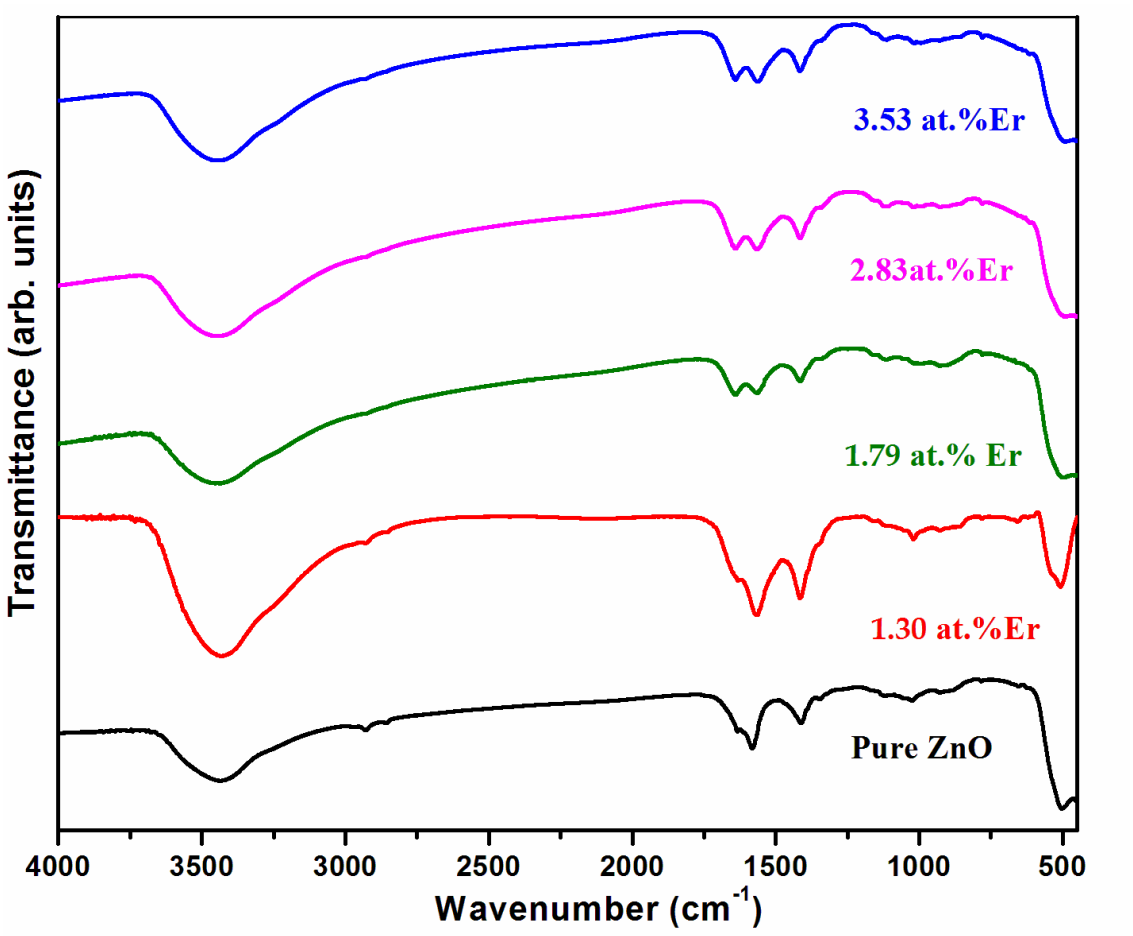

Fig. 3. Fourier transform infrared spectra of as-synthesized pure and Er doped ZnO nanoparticles.

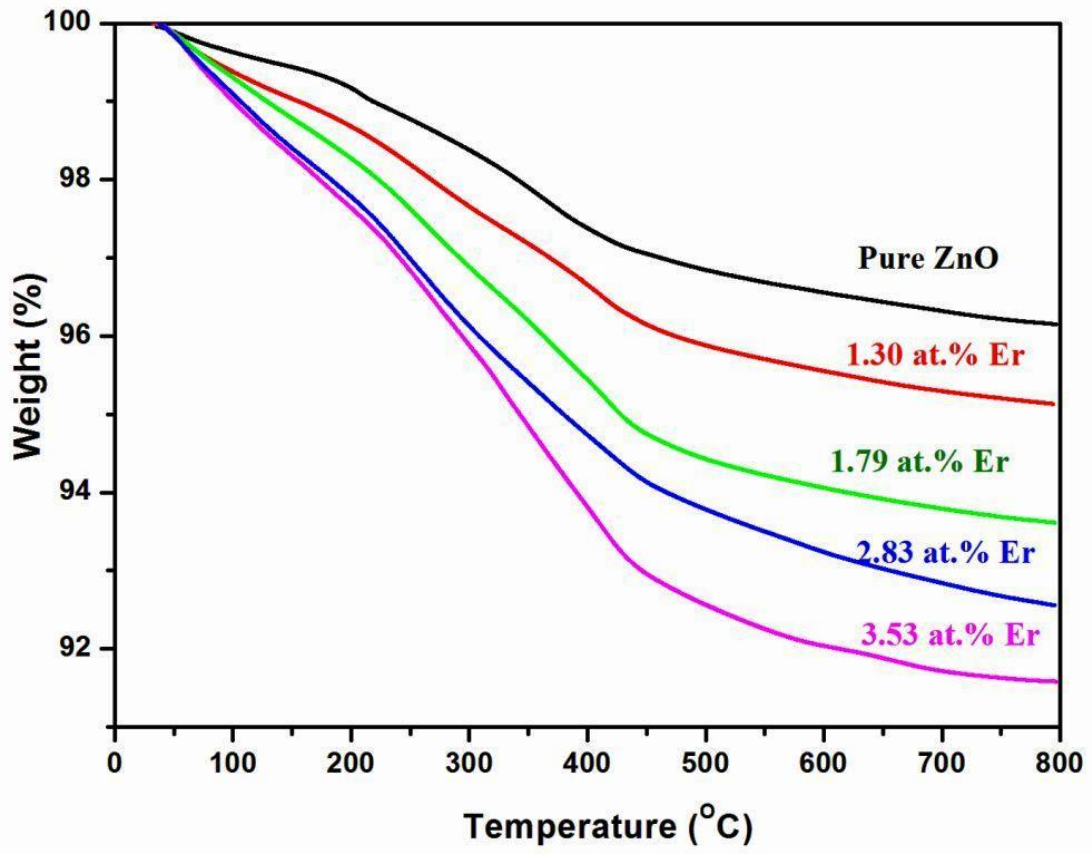

Fig. 4. TGA thermograms of pure and Er doped ZnO nanoparticles.

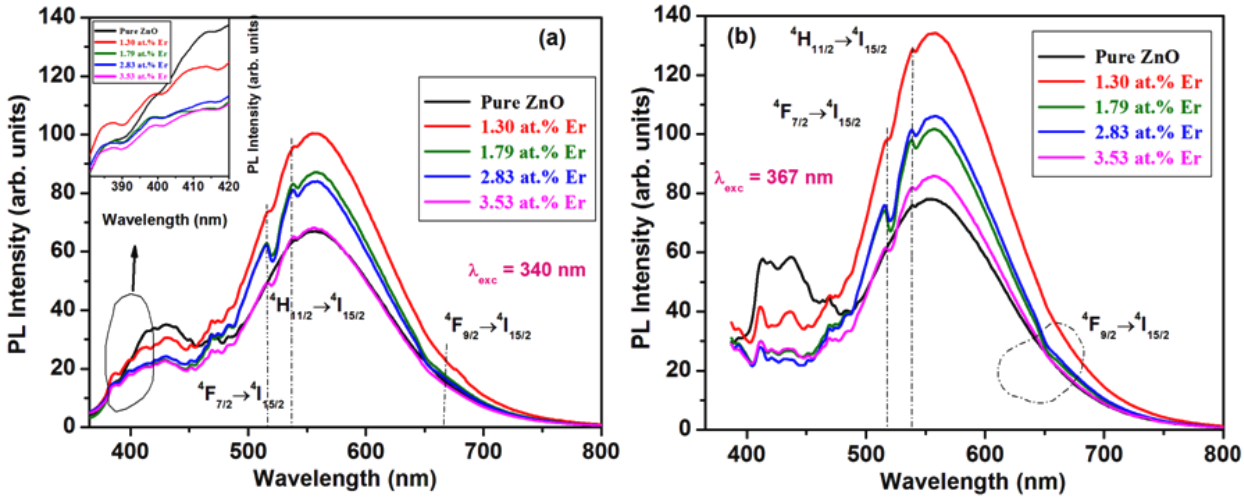

Fig. 5. Photoluminescence spectra of pure and Er doped ZnO nanoparticles with (a) Excitation wavelength 340 nm and (b)Excitation wavelength 367 nm and

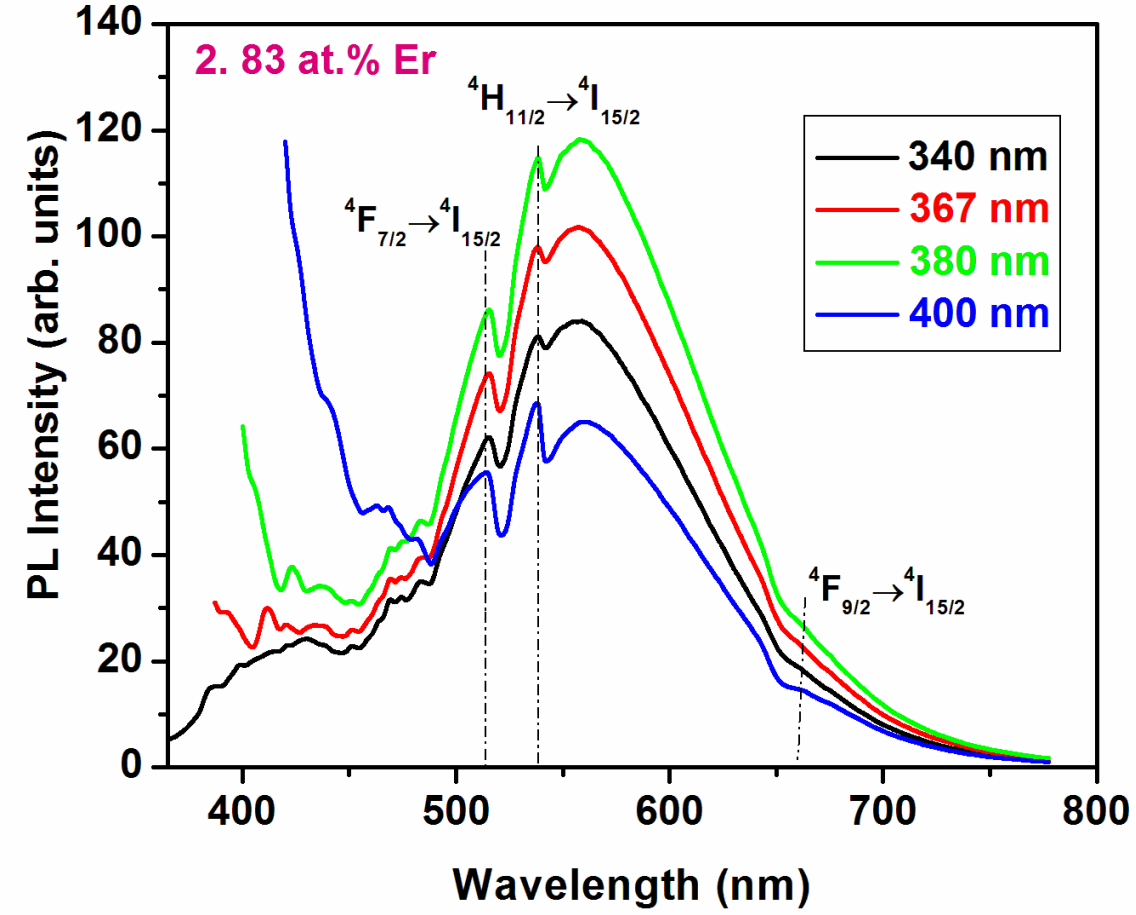

Fig. 6. PL emission spectra of 2.83 at. % of Er doped ZnO nanoparticles with different excitations wavelengths.

Energy Transfer Mechanisms and Dopant-Dependent Luminescence Properties of Er-ZnO Nanoparticles